THE JOURNAL OF BIOLOGICAL CHEMISTRY Vol. 277, No. 28, Issue of July 12, pp. 25640–25648, 2002

A Constitutively Nuclear Form of NFATx Shows Efficient Transactivation Activity and Induces Differentiation of CD4$^+$CD8$^+$ T Cells*

Received for publication, February 25, 2002, and in revised form, April 29, 2002
Published, JBC Papers in Press, May 7, 2002, DOI 10.1074/jbc.M201860200

Yoshiharu Amasaki‡§¶, Satoko Adachi§‖, Yukisato Ishida‖, Makoto Iwata‖, Naoko Arai‡‡, Ken-ichi Arai‡, and Shoichiro Miyatake‡§§¶¶**

From the ‡Department of Molecular and Developmental Biology, Institute of Medical Science, University of Tokyo, Tokyo 108-8639, Japan, the ‖Life Science Research Department, Mitsubishi Kagaku Institute of Life Sciences, Tokyo 194-8511, Japan, the ‡‡Department of Immunology, DNAX Research Institute of Molecular and Cellular Biology, Palo Alto, California 94304-1104, and the §§Department of Immunology, Tokyo Metropolitan Institute of Medical Science, Tokyo 113-8613, Japan

The Ca^{2+} signal facilitates nuclear translocation of NFAT through the dephosphorylation of clustered serine residues in the calcium regulatory domain by the Ca^{2+}/calmodulin-dependent phosphatase calcineurin. The conformation of dephosphorylated NFAT exposes the nuclear localization signal for translocation into the nucleus and masks the nuclear export sequence to keep the protein in the nucleus. It has been reported that deletion of some serine-rich motifs masking the nuclear localization signal results in the translocation of NFAT into the nucleus, but that the nuclear export sequence located at the N terminus also needs to be deleted for NFATx (NFAT4/NFATc3) to exert efficient transactivation function. Here, we report that deletion of the critical serine-rich motifs of NFATx leads to a conformation that efficiently exposes the nuclear localization signal and that has stronger transcription activity compared with the fully activated wild-type protein in the presence of the nuclear export sequence. This also suggests that the regulation of the transactivation domain by phosphorylation observed in NFAT1 may not contribute significantly to the transcription activity of NFATx. The expression of this constitutively nuclear form of NFATx in the CD4$^+$CD8$^+$ T cell line facilitates differentiation into the CD4 single-positive stage upon stimulation with phorbol ester. Our data suggest that NFATx is involved in the regulation of co-receptor expression during differentiation into the CD4 single-positive stage.

One of the outputs of the proximal signaling pathways of the T cell antigen receptor is activation of phospholipase Cγ1. Phospholipase Cγ1 catalyzes phosphatidylinositol 4,5-bisphosphate to produce inositol 1,4,5-triphosphate and diacylglycerol (1). Inositol 1,4,5-triphosphate is a crucial messenger molecule in up-regulating cytoplasmic Ca^{2+} concentrations, whereas diacylglycerol activates the small G protein Ras through binding to the Ras guanyl nucleotide-releasing protein, the hematopoietic cell-specific guanine nucleotide exchange factor, via the diacylglycerol-binding domain and has a role as a protein kinase C activator (2). Protein kinase C also contributes to the activation of Ras. The up-regulation of cytoplasmic calcium leads to the activation of various Ca^{2+}/calmodulin-dependent enzymes, including the phosphatase calcineurin. One of the crucial targets of calcineurin is NFAT (nuclear factor of activated T cells) family members (3, 4). Dephosphorylation of NFAT family proteins results in nuclear translocation (5–7). The activation of Ras and the downstream mitogen-activated protein kinase cascade leads to the activation of AP-1 (activator protein-1). Many genes including those of various cytokines are induced by the collaborative activity of NFAT and AP-1.

NFAT transcription activity is regulated by several steps. One important step is the regulation of intracellular localization. NFAT family members harbor two conserved nuclear localization signals (NLS),[1] one in the calcium regulatory domain and the other in the DNA-binding domain. The location of the nuclear export sequence (NES) has been identified in both NFATx (NFAT4/NFATc3) and NFATc (NFAT2/NFATc1) (8, 9). The NES of NFATx is located within the transactivation domain near the N terminus, whereas the NES of NFATc is mapped near the C terminus of the calcium regulatory domain. The calcium regulatory domains of NFAT family members harbor several conserved motifs containing many serine residues, the phosphorylation of which is regulated by calcineurin and various NFAT kinases (10–12). These serine-rich motifs are the calcineurin-regulated inhibitory sequence (CRI)/serine-rich region (SRR) and three serine-proline (SP) boxes/repeats (SP1, SP2, and SP3), which are located in the C terminus of the CRI/SRR region (13, 14). Deletions or point mutations of serine residues in these conserved motifs result in increased nuclear translocation and transcription activation of the promoters carrying NFAT sites, suggesting that these serine-rich motifs mask NLS (12, 13, 15, 16). In the case of NFATx, removal of the NES in addition to deletion of serine-rich motifs has also been reported to be required to maintain the NFATx protein in the nucleus and for it to exert its transcription activity efficiently

---

* The costs of publication of this article were defrayed in part by the payment of page charges. This article must therefore be hereby marked "*advertisement*" in accordance with 18 U.S.C. Section 1734 solely to indicate this fact.

§ Both authors contributed equally to this work.

¶ Present address: Dept. of Internal Medicine II, Hokkaido University School of Medicine, Sapporo 060-8648, Japan.

** Present address: Div. of Biology, 156-29, California Institute of Technology, Pasadena, CA 91125.

¶¶ To whom correspondence should be addressed: Dept. of Immunology, Tokyo Metropolitan Institute of Medical Science, 3-18-22 Honkomagome, Bunkyo-ku, Tokyo 113-8613, Japan. Tel.: 81-3-5685-6608; Fax: 81-3-5685-6608; E-mail: smiya@rinshoken.or.jp.

[1] The abbreviations used are: NLS, nuclear localization signal(s); NES, nuclear export sequence; CRI, calcineurin-regulated inhibitory sequence; SRR, serine-rich region; SP, serine-proline; PMA, phorbol 12-myristate 13-acetate; mNFAT, murine NFAT; EGFP, enhanced green fluorescent protein; IL, interleukin; EMSA, electrophoretic mobility shift assay; GFP, green fluorescent protein.

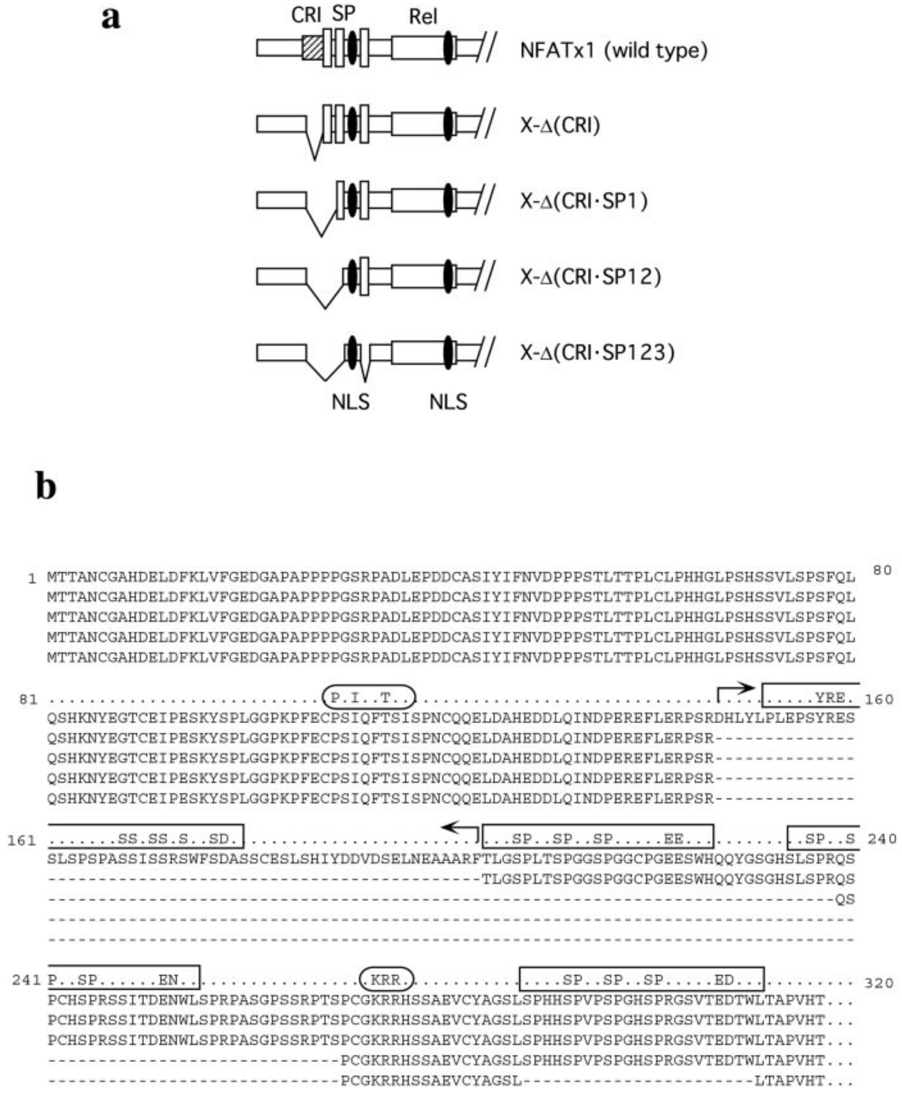

```
  1 MTTANCGAHDELDFKLVFGEDGAPAPPPPGSRPADLEPDDCASIYIFNVDPPPSTLTTPLCLPHHGLPSHSSVLSPSFQL  80
    MTTANCGAHDELDFKLVFGEDGAPAPPPPGSRPADLEPDDCASIYIFNVDPPPSTLTTPLCLPHHGLPSHSSVLSPSFQL
    MTTANCGAHDELDFKLVFGEDGAPAPPPPGSRPADLEPDDCASIYIFNVDPPPSTLTTPLCLPHHGLPSHSSVLSPSFQL
    MTTANCGAHDELDFKLVFGEDGAPAPPPPGSRPADLEPDDCASIYIFNVDPPPSTLTTPLCLPHHGLPSHSSVLSPSFQL
    MTTANCGAHDELDFKLVFGEDGAPAPPPPGSRPADLEPDDCASIYIFNVDPPPSTLTTPLCLPHHGLPSHSSVLSPSFQL

 81 ............................P.I..T.........................................YRE. 160
    QSHKNYEGTCEIPESKYSPLGGPKPFECPSIQFTSISPNCQQELDAHEDDLQINDPEREFLERPSRDHLYLPLEPSYRES
    QSHKNYEGTCEIPESKYSPLGGPKPFECPSIQFTSISPNCQQELDAHEDDLQINDPEREFLERPSR--------------
    QSHKNYEGTCEIPESKYSPLGGPKPFECPSIQFTSISPNCQQELDAHEDDLQINDPEREFLERPSR--------------
    QSHKNYEGTCEIPESKYSPLGGPKPFECPSIQFTSISPNCQQELDAHEDDLQINDPEREFLERPSR--------------
    QSHKNYEGTCEIPESKYSPLGGPKPFECPSIQFTSISPNCQQELDAHEDDLQINDPEREFLERPSR--------------

161 .......SS.SS.S..SD.........................SP..SP..SP.....EE...........SP..S 240
    SLSPSPASSISSRSWFSDASSCESLSHIYDDVDSELNEAAARFTLGSPLTSPGGSPGGCPGEESWHQQYGSGHSLSPRQS
    -------------------------------------------TLGSPLTSPGGSPGGCPGEESWHQQYGSGHSLSPRQS
    ------------------------------------------------------------------------------QS
    --------------------------------------------------------------------------------
    --------------------------------------------------------------------------------

241 P..SP......EN.................KRR...............SP..SP..SP.....ED.............. 320
    PCHSPRSSITDENWLSPRPASGPSSRPTSPCGKRRHSSAEVCYAGSLSPHHSPVPSPGHSPRGSVTEDTWLTAPVHT...
    PCHSPRSSITDENWLSPRPASGPSSRPTSPCGKRRHSSAEVCYAGSLSPHHSPVPSPGHSPRGSVTEDTWLTAPVHT...
    PCHSPRSSITDENWLSPRPASGPSSRPTSPCGKRRHSSAEVCYAGSLSPHHSPVPSPGHSPRGSVTEDTWLTAPVHT...
    -----------------------------PCGKRRHSSAEVCYAGSLSPHHSPVPSPGHSPRGSVTEDTWLTAPVHT...
    -----------------------------PCGKRRHSSAEVCYAGSL------------------------LTAPVHT...
```

FIG. 1. **Deletion constructs of NFATx1 used in this study.** Both a schematic diagram of various NFATx deletion constructs (*a*) and an alignment of the deleted amino acid residues of each construct (*b*) are shown.

(8). In the case of NFAT1 (NFATp/NFATc2), the nuclear localization of the protein by exposing the NLS results in partial transcription activity (16). Phosphorylation of specific serine residues is also required within the transcription activation domain for the complete transcription activity of NFAT1. In this work, a constitutively nuclear localizing NFATx mutant with full transcription activity stronger than that of the wild-type protein in the absence of Ca^{2+} signals was created by serially deleting the conserved serine-containing motifs of NFATx. This mutant harbors an intact NES, indicating that complete activation of nuclear import activity can overcome nuclear export activity to facilitate efficient transcription. Furthermore, in contrast to NFAT1, the regulation of the transcription activation domain by phosphorylation may not be required for the complete transcription activity of NFATx.

NFAT family proteins have been suggested to play crucial roles in the development of T cells in thymus (17). Utilizing the calcineurin inhibitors cyclosporin and FK506, the activity of calcineurin in CD4$^+$CD8$^+$ thymocytes has been shown to be important for positive selection and/or negative selection (18–23). Due to the critical role of NFAT family proteins in the activation of mature T cells, it has been speculated that the major targets of calcineurin in thymocytes are NFAT family proteins. Among NFAT family members, NFATx is most highly expressed in CD4$^+$CD8$^+$ cells (24), and NFATx-defective mice show reduced numbers of CD4$^+$CD8$^+$ cells (25). This reduction of the CD4$^+$CD8$^+$ cell population is presumably due to the reduced level of anti-apoptotic Bcl-2 protein expression, leading to their susceptibility to apoptosis (25). This indicates that the role of NFATx in thymocytes is to up-regulate Bcl-2 expression in response to the selecting signal to facilitate thymocyte survival. RLm6 (RL male 6) cells, a CD4$^+$CD8$^+$ T lymphoma, and CD4$^+$CD8$^+$ thymocytes differentiate into CD4 single-positive cells upon phorbol 12-myristate 13-acetate (PMA) and calcium ionophore treatment (26, 27). We show that when the constitutively nuclear NFATx mutant was introduced into this cell line, differentiation into the CD4 single-positive stage was induced in the presence of PMA alone, suggesting that NFATx plays an important role in the positive selection by regulating the expression pattern of CD4 and CD8 co-receptors.

EXPERIMENTAL PROCEDURES

Cells—COS-7 cells were grown in Dulbecco's modified Eagle's medium supplemented with 10% heat-inactivated fetal calf serum, and Jurkat cells were grown in RPMI 1640 medium supplemented with 5% fetal calf serum at 37 °C in an atmosphere containing 5% CO_2 (28). RLm6 cells, an x-ray-induced CD4$^+$CD8$^+$ T cell leukemia line from BALB/c mice, were cultured in complete Dulbecco's modified Eagle's medium supplemented with 10% fetal calf serum and antibiotics (29). RLm6-ΔCN, an RLm6 transfectant expressing the Ca^{2+}-independent form of calcineurin, was obtained as previously described (26).

Plasmids—pMEmNFATx1 is a mammalian expression plasmid that has been previously described (30). This plasmid contains full-length murine NFATx1 (mNFATx1) cDNA under the control of the SRα pro-

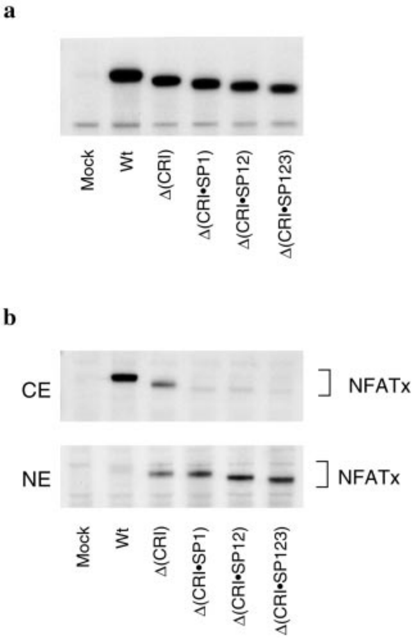

FIG. 2. **Protein expression and subcellular localization of mutant NFATx1 proteins expressed in COS-7 cells.** *a*, detection of mutant NFATx proteins expressed in whole cell extracts from COS-7 cells transfected with various mutant NFATx constructs by immunoblotting; *b*, detection of mutant NFATx proteins in fractionated cytoplasmic (*CE*) or nuclear (*NE*) extracts from transfected COS-7 cells by immunoblotting. *Wt*, wild-type.

moter in the pME18S vector and was used for the construction of plasmids containing various deletions in NFATx1 based on standard recombinant techniques and PCR methods. To construct pMEmX-Δ(CRI) and pMEmX-Δ(CRI·SP12), the *Xba*I-*Sca*I fragment in mNFATx1 cDNA (positions 440–995) was replaced by PCR fragments generated from pMEmNFATx1, yielding in-frame truncation at positions 446–616 and 446–814, respectively. pMEmX-Δ(CRI·SP1) was constructed by removing an *Xba*I-*Avr*II fragment (positions 440–716), followed by direct self-ligation. pMEmX-Δ(CRI·SP12) was processed for further truncation by replacing the 186-bp *Xba*I-*Sca*I fragment in this plasmid with a 117-bp PCR-generated fragment derived from pMEmNFATx1, generating pMEmX-Δ(CRI·SP123) containing an additional truncation corresponding to positions 869–937 in the mNFATx1 sequence. Nucleotide sequences of junctions and PCR-derived fragments were verified in all of the plasmids by DNA sequencing. Deduced amino acid sequences in the corresponding regions of the plasmids are summarized in Fig. 1. In particular experiments, the carboxyl-terminal domains of wild-type or truncated NFATx1 constructs (corresponding to positions 2116–3235 in mNFATx1) were replaced with a 720-bp DNA fragment encoding enhanced green fluorescent protein (EGFP) cDNA, excised from pEGFP-N1 (CLONTECH, Palo Alto, CA) by *Apa*I and *Not*I. Plasmid pNFAT72-Luc contains the luciferase reporter gene under the control of three of the murine interleukin (IL)-2 promoter NFAT sites (positions −290–261) (31). pRL-SV40, a co-reporter plasmid for the Dual-Luciferase™ reporter assay, was purchased from Promega (Madison, WI). pMKITmNFATx and pMKITmNFAT-Δ(CRI·SP12) contain wild-type mNFATx cDNA from pMEmNFATx1 and mNFATx lacking CRI, SP1, and SP2 from pMEmX-Δ(CRI·SP12), respectively.

Transfection, Cell Stimulation, Cell Extracts, and Western Blotting—Transient transfection in COS-7 and Jurkat cells was carried out by a DEAE-dextran method as described previously (24, 28). RLm6 cell transfectants stably expressing wild-type or truncated forms of NFATx1 were generated as follows. *Eco*RI-*Xho*I fragments encoding the full-length or truncated forms of NFATx1 cDNA were subcloned into a mammalian expression vector (pMKIT-Neo) from which the *Mlu*I fragment had been excised. pMKITmNFATx, pMKITmNFAT-Δ(CRI), and pMKITmNFAT-Δ(CRI·SP12) were thus obtained. The linearized constructs were prepared by digestion with *Nlu*I. RLm6 cells were transfected with the linearized constructs or control pMKIT-Neo by electroporation and selected as previously described (24). RLm6 or its transfectants were stimulated with PMA (Sigma) and/or ionomycin as previously described (24) in the presence or absence of FK506 as indicated.

To prepare the whole cell extracts, cells were harvested at 48 h, rinsed with phosphate-buffered saline, and then lysed with radioimmune precipitation assay buffer containing protease and phosphatase inhibitors as described (32). The lysates were rotated for 30 min at 4 °C and centrifuged at 15,000 rpm for 15 min to remove debris. Cytosolic and nuclear extracts from transfected COS-7 cells were prepared as described previously (28). These lysates were separated by SDS-PAGE, transferred to nylon membrane, and blotted with rabbit anti-NFATx antibody X-75 (13), followed by detection using an ECL™ kit (Amersham Biosciences).

Luciferase Assay—Jurkat cells were maintained in RPMI 1640 medium supplemented with 5% heat-inactivated fetal calf serum, antibiotics, and 1 mM L-glutamine at 37 °C in a humidified atmosphere containing 5% CO_2. Luciferase assay was carried out according to the procedure described previously (13), with minimal modification. Briefly, 3×10^6 Jurkat cells were transfected with a pME18S-based expression vector (15 μg) and the pNFAT72-Luc reporter plasmid (3 μg) (31). For the control to monitor the efficiency of transfection, the pRL-SV40 *Renilla* luciferase reporter plasmid (0.25 μg) was also included for transfection. After 40 h of incubation, cells were stimulated with 20 ng/ml PMA with or without 0.5 mM A23187(Calbiochem) for 8 h at 37 °C in a humidified atmosphere containing 5% CO_2, and then the cells were harvested.

Electrophoretic Mobility Shift Assay (EMSA)—EMSAs were conducted using a double-strand oligonucleotide probe containing the distal NFAT site from the human IL-2 promoter with 1 μg of transfected COS-7 cytosolic or whole cell extracts. Procedures for EMSAs and the double-strand oligonucleotides used in this study have been described previously (24).

Intracellular [Ca^{2+}] Measurement—Cultured cells were incubated with 3 μM fura-2/AM (Texas Fluorescence Labs Inc., Austin, TX) for 20 min. Using a fluorometer (CAF-100, Jasco, Tokyo, Japan), the emitted fluorescence (520 nm) in response to alternate pulses of excitation light at 340 and 380 nm was monitored for 15 min. Triton X-100 (0.1%) and EGTA (10 mM) were successively added to the cell suspension to determine the intracellular Ca^{2+} concentration according to an equation with a K_d value of 224 nM as described (33). In all tested cells under unstimulated conditions, the intracellular Ca^{2+} concentration determined by the fura-2 method was ~150 nM (range of 134–170 nM).

RESULTS

Preferential Nuclear Localization of NFATx Proteins Harboring Deletions of the CRI/SRR, SP1, SP2, and SP3 Motifs—It has been shown that the calcium regulatory domain includes critical motifs that regulate subcellular localization of NFAT proteins. In the case of NFATx, we have previously shown that when the CRI/SRR motif in its calcium regulatory domain was truncated, the NFATx protein showed not only enhanced nuclear localization, but also transactivation upon PMA-alone stimulation (13). However, the extent of transactivation by CRI/SRR-deleted NFATx upon PMA-alone stimulation was very limited compared with that upon PMA plus calcium ionophore stimulation. This prompted us to further modify the calcium regulatory domain to create constitutively active forms that show strong transcription activity.

Among conserved motifs in calcium regulatory domain, SP motifs (SP*XX*SP*XX*SP*XXXXX*(E/D)(E/D)) adjacent to the CRI/SRR domain are short sequences that have been suggested to be a target of stimulation-dependent serine phosphorylation/dephosphorylation of NFAT proteins (5–7, 15). We first examined the function of NFATx molecules by serial truncation of the SP motifs in addition to CRI/SRR. Among the multiple isoforms of NFATx, NFATx1 is the one that is predominantly expressed in human and murine thymuses that might be involved in thymocyte differentiation (30, 31). In this study, murine NFATx1 was used for experiments in view of its application in murine cells. The residues of the CRI/SRR domain and SP motifs are almost completely identical between human and mouse NFATx homologs (30). We first truncated the amino acid residues corresponding to the CRI/SRR region of murine NFATx. In addition to this construct, designated X-Δ(CRI), we generated additional constructs that had serially truncated SP

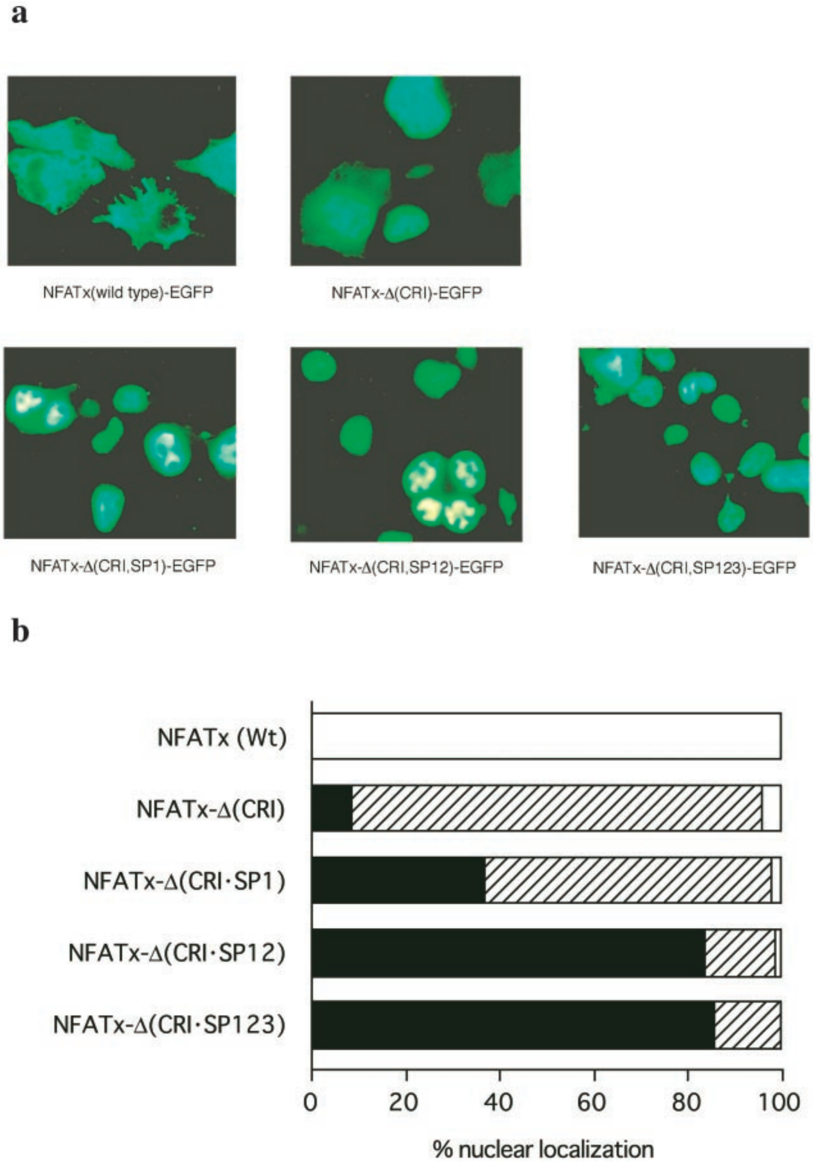

FIG. 3. **Enhanced nuclear localization of mutant NFATx proteins fused to EGFP in unstimulated COS-7 cells.** *a*, microscopic display of wild-type (*Wt*) and mutant EGFP-fused NFATx1 constructs expressed in COS-7 cells; *b*, numerical representation of the nuclear localization of EGFP-fused NFATx mutants. The percentages of cells with nuclear fluorescence (*open bars*), both nuclear and cytoplasmic fluorescence (*hatched bars*), and cytoplasmic fluorescence (*closed bars*) out of the 200 cells positive for EGFP were microscopically determined. Averages of three independent experiments are displayed.

motifs (Fig. 1, *a* and *b*). Residues covering SP1 and SP1/2 were serially truncated in X-Δ(CRI·SP1) and X-Δ(CRI·SP12), respectively. In X-Δ(CRI·SP123), SP3 was further truncated from X-Δ(CRI·SP12), leaving intact amino acid residues between SP2 and SP3 that have been predicted to contain an NLS (6, 13, 15).

The protein expression levels and subcellular distribution of these NFATx mutants were examined by transfecting the CRI/SP-truncated constructs into COS-7 cells, taking advantage of the efficient separation of nuclear and cytoplasmic protein fractions from these cells. When crude whole cell extracts from the transfected cells were subjected to immunoblotting (Fig. 2*a*), the wild-type or mutant NFATx protein was detected using specific anti-NFATx antiserum, with different molecular sizes being consistent with the different lengths of truncation. It was also notable that truncated molecules, especially in the case of X-Δ(CRI·SP123), showed reduced amounts of protein expression compared with wild-type NFATx.

To examine the subcellular distribution of the mutant NFATx1 proteins, we next prepared extracts from nuclear and cytoplasmic fractions from COS cells transfected with these constructs, followed by immunoblot analysis. As expected, the wild-type NFATx protein showed highly selective cytoplasmic sequestration (Fig. 2*b*, *second lane*). In contrast, when using cytoplasmic and nuclear extracts from cells transfected with X-Δ(CRI), truncated NFATx protein was detected both in cytoplasmic and nuclear fractions (Fig. 2*b*, *third lane*), consistent with observations in human NFATx1 protein (13). However, when one or more SP motifs were truncated, the resultant NFATx proteins were detected preferentially in the nuclear fraction, but barely in the cytoplasmic fraction (Fig. 2*b*, *fourth* through *sixth lanes*). These results are consistent with the notion that SP motifs, in addition to the CRI/SRR region, are critical for the regulation of subcellular localization of the NFATx protein (15, 16).

To analyze the intracellular distribution of the wild-type and mutant NFATx proteins in individual cells, we generated GFP-fused constructs of NFATx mutants in which the carboxyl-terminal domain of each NFATx mutant was replaced with cDNA encoding GFP (Fig. 3*a*). When COS cells were transfected with the wild-type NFATx-GFP plasmid, the resultant NFATx-GFP protein was localized completely in the cytoplasm of transfected COS cells (Fig. 3*a*, *upper left panel*). In contrast, X-Δ(CRI) showed nuclear distribution, whereas some fluorescence was also observed in the cytoplasm (Fig. 3*a*, *upper right panel*). When X-Δ(CRI·SP1) was transfected, increased nuclear distribution was observed (Fig. 3*a*, *lower left panel*). Interestingly, transfection of the NFATx-GFP mutant lacking SP1 and

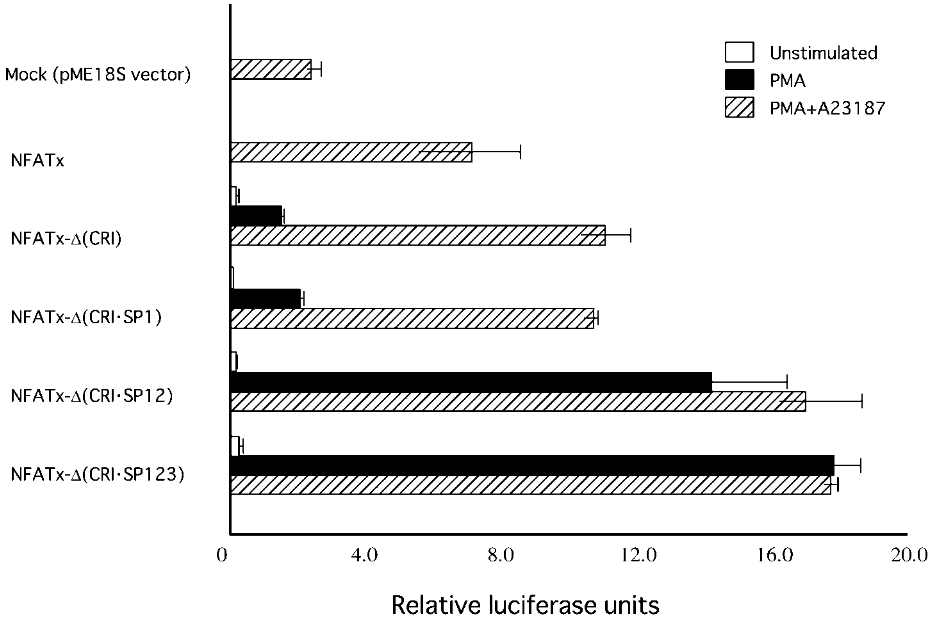

FIG. 4. **NFAT transactivation by various NFATx mutants upon PMA-alone or PMA plus A23187 stimulation.** Jurkat cells were transiently transfected with various mutant NFATx1 constructs or the empty pME18S vector with the pNFAT72-Luc reporter plasmid. Cells were incubated for 40 h after transfection and then stimulated for 8 h and harvested, followed by Dual-Luciferase assay analyses. The data represent averages of three independent experiments.

SP2 or all three SP motifs resulted in highly selective nuclear localization (Fig. 3*a*, *lower middle* and *right panels*). These results were also obtained when cells were counted for cytoplasmic/nuclear fluorescence (Fig. 3*b*). Thus, serial truncation of SP motifs enhances nuclear localization of the NFATx protein.

CRI/SP-truncated NFATx Proteins Are "Conditional" Mutants Showing Efficient Transactivation upon PMA-alone Stimulation—Based on the observation that CRI-truncated NFATx shows PMA-alone-induced transactivation (13), we examined the activities of these NFATx mutants in inducing calcium ionophore-independent transactivation (Fig. 4). Expression plasmids for wild-type or mutant NFATx proteins were transfected into Jurkat T cells with a reporter plasmid carrying three tandem copies of NFAT/AP-1 sites, followed by stimulation using PMA or PMA plus A23187. Jurkat cells transfected with the control pME18S plasmid showed weak NFAT transactivation upon stimulation with PMA plus A23187, which might reflect endogenous NFAT activity. When cells were transfected with the plasmid encoding wild-type NFATx, increased NFAT activity was observed in the presence of both PMA and A23187 (Fig. 4, *second bar*). In contrast, when cells were transfected with the plasmid encoding X-Δ(CRI), transactivation driven through NFAT sites was observed even after PMA-alone stimulation, despite the low activity (Fig. 4, *third group of bars*). These results are consistent with our previous observations in human NFATx (13). Moreover, truncation of SP motifs dramatically increased PMA-alone-induced transactivation of mutant NFATx constructs. When SP1 was truncated in addition to CRI/SRR, transactivation was increased (Fig. 4, *fourth group of bars*). However, when SP1 and SP2 or all three SP motifs were truncated, these mutant NFATx constructs induced significantly increased transactivation upon PMA-alone stimulation, comparable to the stimulation with both PMA plus A23187 (Fig. 4, *fifth* and *sixth groups of bars*). The activities of these mutants were much stronger than the wild-type activity. Thus, CRI/SP deletion in NFATx results not only in increased nuclear localization, but also in efficient transactivation in the absence of calcium/calcineurin signaling.

Modified DNA Binding of CRI-truncated NFATx Mutants—The increased transactivation by CRI/SP-truncated mutants of NFATx could be partially explained by their increased nuclear distribution (Figs. 2 and 3). However, increased transactivation might also be caused by the altered affinity of DNA binding by mutant NFAT molecules. We therefore tested protein-DNA binding of mutant NFATx using extracts from transfected COS-7 cells. Because subcellular distribution was very different among various NFATx mutants (Fig. 2), whole cell extracts from transfected COS cells were used for the EMSA analysis. As shown in Fig. 5*a*, whole cell extract from COS-7 cells transfected with wild-type NFATx showed an NFAT-DNA-binding complex that was comparable to the reconstituted NFAT-DNA complex in cytosolic extract with NFATx1 and exogenous AP-1 (HeLa nuclear extract) (34). NFATx-DNA contained two major bands. Studies using competitor oligonucleotides indicated that the upper slow-migrating band represents an NFAT-AP-1 complex, whereas the lower fast-migrating band represents NFAT without AP-1, consistent with previous studies (24, 35).

NFAT-DNA complexes in cell extracts from COS cells transfected with mutant NFATx molecules were then examined. As shown in Fig. 5*b*, when extracts from mutant NFAT transfectants were tested, all extracts showed NFAT-DNA-binding activities containing two major protein-DNA complexes. Interestingly, when the extract with X-Δ(CR1) was tested, both the upper and lower complexes appeared with higher intensities than in the wild-type NFATx transfectants (Fig. 5*b*, *lanes 1* and *2*). In addition, the lower complex appeared with slower mobilities than in the wild-type NFATx transfectant (Fig. 5*b*, *lanes 1* and *2*). Because the amount of the expressed X-Δ(CRI) protein in transfected COS cell extracts was less than that of wild-type NFATx (Fig. 2*a*), the increased NFAT-DNA binding of X-Δ(CRI) may be attributable to modified DNA-binding affinity. Other mutants showed two similar NFAT-DNA complexes with CRI-truncated mutants with slight mobility differences that would represent different molecular sizes. X-Δ(CRI·SP123) showed reduced intensities of the NFAT protein-DNA complex, which would be due to reduced protein expression in COS cells (Fig. 2*a*). Among CRI/SP-truncated mutants, the extent of SP deletion did not appear to increase the intensity of the NFAT-DNA complex, suggesting that truncation of CRI (but not SP motifs) affects the DNA-binding affinities of these mutants.

CRI/SP-deleted NFATx Mutants Function as Conditionally Active Mutants Able to Induce Differentiation of CD4$^+$CD8$^+$ T Cells upon PMA-alone Stimulation—We wondered whether NFATx plays an important role in thymocyte positive selection. Thus, we used these conditionally active mutants of NFATx to

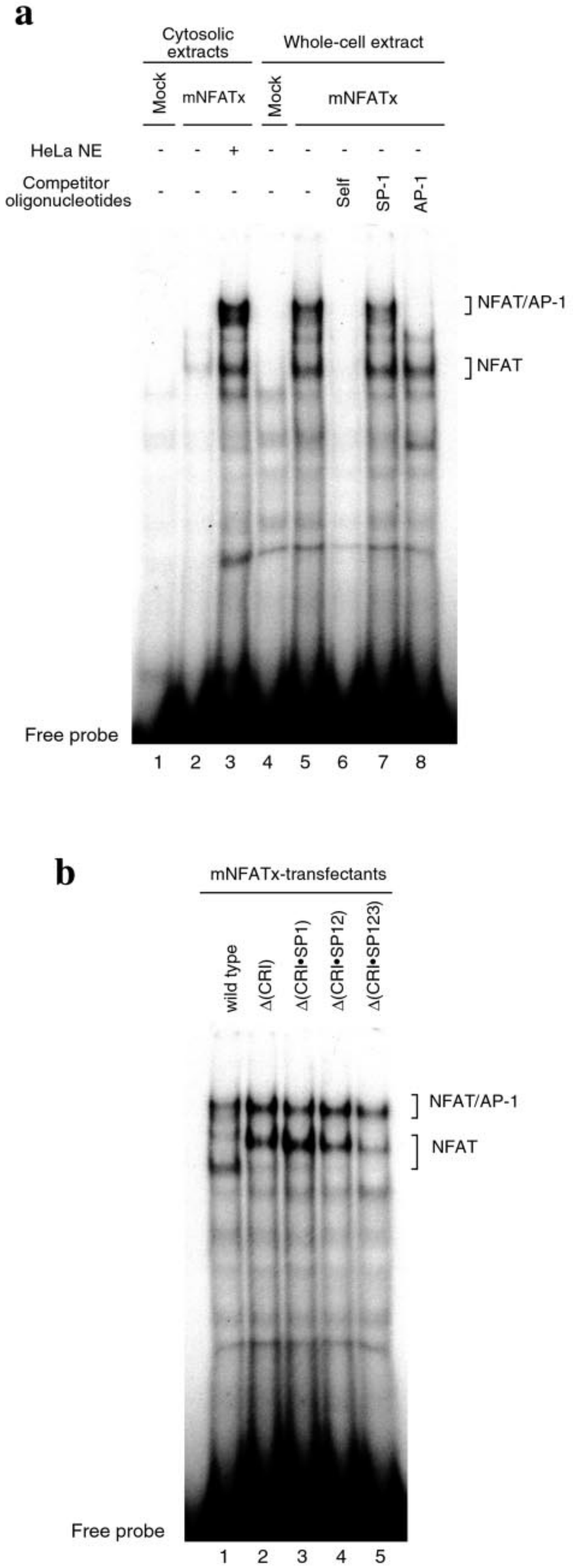

FIG. 5. **Comparison of NFAT protein-DNA binding of various NFATx1 constructs expressed in COS-7 cells by EMSA.** The DNA-binding activities of the cytosolic and whole cell extracts of NFATx-transfected COS cells were compared by EMSA analysis. The nuclear extract (*NE*) of HeLa cells contained AP-1 activity (*a*). Sequence-specific DNA-binding activities of the whole cell extracts prepared from wild-type and various mutant NFATx plasmid-transfected COS cells were analyzed (*b*).

determine whether NFATx contributes to the differentiation of a CD4$^+$CD8$^+$ T cell line. Wild-type or mutant NFATx cDNAs were ligated to the pMKIT-Neo expression vector, and the resultant plasmids were transfected into the RLm6 T cell line, representing the CD4$^+$CD8$^+$ stage of thymocytes. RLm6 is an x-ray-induced CD4$^+$CD8$^+$ T cell line (29) that becomes CD4 single-positive (26) and acquires the CC chemokine receptor CCR7 (36) upon calcium ionophore ionomycin/PMA stimulation. pMKITmNFATx, pMKITmNFATx-Δ(CRI), and pMKITmNFATx-Δ(CRI·SP12) were used for generating stable transfectants, and 5, 6, and 10 gentamycin-resistant clones were obtained, respectively (Table I). All of the transfectants retained the CD4$^+$CD8$^+$ phenotype without stimulation and developed the CD4 single-positive phenotype after ionomycin/PMA stimulation, as in the case of parental cells. However, in the case of cells transfected with CRI/SP-truncated NFATx, some of the cells showed phenotypic changes to CD4 single-positive even after PMA-alone stimulation (Table I). Representative results of the experiments are shown in Fig. 6. Similar to the case of ΔCN, the calcium-independent form of calcineurin (26), some RLm6 cells transfected with X-Δ(CRI·SP12) responded to PMA-alone stimulation and became CD4 single-positive or CD4$^+$CD8^{low}. Strikingly, the PMA-induced differentiation of X-Δ(CRI·SP12)-transfected cells was resistant to the action of FK506, whereas that of ΔCN-transfected cells was markedly inhibited by FK506. FK506 is a well known inhibitor of thymocyte positive selection (18, 22, 23) and can inhibit calcineurin activity even in its calcium-independent form encoded by ΔCN (37).

To confirm that the phenotypic change in RLm6 transfectants was induced by the action of expressed NFATx and not by an alteration of intracellular Ca^{2+} mobilization, we measured the intracellular Ca^{2+} concentration of transfectants. As shown in Table II, there was no significant correlation between the intracellular Ca^{2+} levels of RLm6 transfectant cells and the phenotypic changes in the cells.

DISCUSSION

The mechanism of nuclear transport of NFAT family proteins has been extensively studied. Typical NLS sequences are present in both the calcium regulatory domain and the Rel similarity domain, which is required for DNA binding. The location of the NES has been mapped in NFATc and NFATx, but at different positions (8, 9). Conserved motifs in the calcium regulatory domain (CRI/SRR, SP1, SP2, and SP3) contain many serine residues, most of which are phosphorylated in unstimulated cells (16). The calcium signal dephosphorylates these serine residues through the activation of calcineurin, leading to a conformational change in the calcium regulatory domain to expose NLS and to induce nuclear translocation (15, 16, 38). We have previously shown that deletion of the CRI/SRR domain makes some of the NFATx protein localize in the nucleus (13, 30). Here, we show that the additional serial deletion of SP motifs in addition to CRI/SRR induced more striking nuclear localization. Deletion of CRI/SRR, SP1, and SP2 showed that nearly 90% of cells harbored NFATx completely in the nucleus, in contrast to deletion of only CRI/SRR, which gave only ~10%. Further deletion of SP3 did not contribute much to the increased extent of nuclear localization. Transcription activity in the presence of PMA measured by the reporter plasmid carrying the NFAT/AP-1 composite site from the IL-2 gene was proportional to the extent of nuclear localization. Deletion of CRI/SRR, SP1, and SP2 resulted in maximal activity upon PMA stimulation, which was higher than that of wild-type NFATx in the presence of both PMA and ionomycin. Again, further deletion of SP3 did not show much additional effect on transcription activity. Zhu and McKeon (8) have re-

TABLE I

Phenotypic changes in RLm6 cells transfected with full-length or truncated NFATx upon stimulation

Construct	Established clone numbers[a]	CD4 single-positive differentiation upon stimulation[b]	
		PMA alone	PMA + ionomycin
pMKITmNFATx	5	0 (0%)	5 (100%)
pMKITmNFATx-Δ(CRI)	6	2 (33%)	6 (100%)
pMKITmNFATx-Δ(CRI · SP12)	10	8 (80%)	10 (100%)

[a] RLm6 cells were transfected with full-length or truncated NFATx, and gentamycin-resistant clones were obtained.

[b] Transfectant clones were stimulated with 0.2 ng/ml PMA alone or with a combination of 0.2 ng/ml PMA and 0.2 μg/ml ionomycin for 48 h and then analyzed for CD4/CD8 expression.

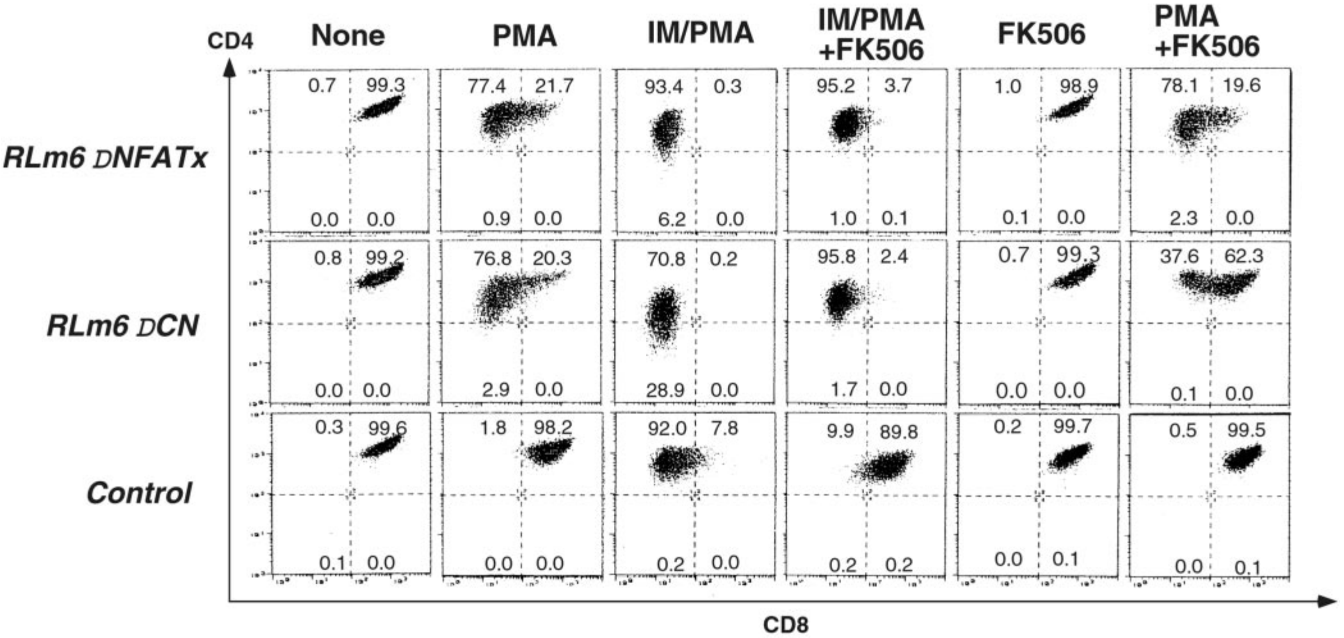

FIG. 6. **Stimulation-dependent phenotypic changes in the RLm6 T cell line transfected with various NFATx constructs.** Stable transfectants with NFATx-Δ(CRI·SP12) (*Lm6 DNFATx*), ΔCN (*RLm6 DCN*), and the control vector (*Control*) were stimulated under various conditions for 48 h, and the expression of CD4 and CD8 co-receptors was analyzed by flow cytometry. The concentrations of PMA, ionomycin (*IM*), and FK506 were 0.2 ng/ml, 0.2 μg/ml, and 10 nM, respectively.

TABLE II

Intracellular Ca^{2+} levels in RLm6 cells transfected with truncated forms of NFATx

RLm6 and its transfectants were incubated with fura-2/AM. After washing, the cells were analyzed for intracellular Ca^{2+} levels by measuring fluorescence intensity. ND, not done.

Transfected DNA	Intracellular Ca^{2+} level	
	Exp. 1	Exp. 2
	nM	
None	143.7	ND
pMKIT-Neo	169.8	134.4
pMKITmNFATx-Δ(CRI · SP12)	165.8	153.9

ported that the nuclear export activity has to be shut off in order for NFAT to stay in the nucleus and to exert its transcription activity. They showed that deletion of the region containing SP1 results in nuclear localization without a calcium signal, although this mutant cannot activate transcription efficiently due to the presence of the NES located in the N terminus. The presence of the NES inhibits the prolonged localization of the NFAT protein in the nucleus. Deletion of the NES in addition to the SP1-containing region is required for NFATx to stay in the nucleus for sufficient time to activate transcription. The X-Δ(CRI·SP12) mutant of NFATx retains the complete NES that Zhu and McKeon mapped, but this mutant showed strong transcription activity upon PMA treatment. In our experiments, deletion of the SP1 region resulted in only a small portion of cells with nuclear localization. Furthermore, the NES mapped by Zhu and McKeon overlaps with the transactivation domain of NFATx. Thus, when the NES is deleted, part of the transcription activation domain is removed. The X-Δ(CRI·SP12) mutant retains an intact NES, but also retains all of the transactivation domain located in the N terminus; it is therefore presumably efficiently imported into the nucleus and induces transcription despite the nuclear export activity mediated through the NES. All this suggests that the balance of nuclear import and export activities, in addition to the sum of the strength of all of the transcription activation domains, contributes to the overall transcription activity of NFATx.

In the presence of PMA, X-Δ(CRI·SP12) gave strong transcription activity, which was stronger than that of the wild-type protein fully activated. Rao and co-workers (16) have reported that a mutant of NFAT1 with alanine replacement of all serine residues in the CRI/SRR, SP1, SP2, and SP3 motifs with a fused NLS derived from SV40 T antigen shows almost complete nuclear localization and strong transcription activity in the presence of AP-1. However, the transcription activity of this mutant is still weaker than that of the wild-type protein fully activated. They then showed that the serines in the SSPS motif located in the transactivation domain very close to the N terminus are phosphorylated upon stimulation. Furthermore, a Gal4 fusion protein with this N-terminal region showed stimulation-dependent transcription activation, in which these serine residues played a crucial role. The transactivation domains located in the N terminus are not conserved among NFAT family members. The SSPS motif is not present in this region of NFATx. Thus, in contrast to NFAT1, NFATx can have full transcription activity without such a mechanism. The kinase that phosphorylates the SSPS motif of NFAT1 has not been identified, but an interesting possibility is that in cells that have little or no activity of this kinase, NFATx may play a more dominant role among NFAT family members, especially for genes with promoters harboring AP-1-independent regulatory regions. This could be one of the mechanisms that contributes to the functional differences of each NFAT family protein. Another interpretation for this difference between NFATx and NFAT1 might be the difference of the promoters used to measure NFAT activity in these experiments. Rao and co-workers used the IL-13 promoter to measure NFAT1 activity, whereas we used the promoter with the NFAT/AP-1 composite site from IL-2.

NFAT family proteins have been shown to play important roles in T cell development in thymus. NFAT proteins are important signaling molecules that mediate positive selection. NFAT family proteins appear to contribute successively to thymocyte differentiation (34). There are some reports suggesting that NFAT proteins are also involved in negative selection, although this is a controversial issue (19–21, 39). Recently, the important role of NFAT in β selection has been reported (40). However, all these reports utilized a calcineurin inhibitor (cyclosporin or FK506) to analyze the involvement of NFAT proteins. We have previously reported that NFATx is the major subtype in the $CD4^+CD8^+$ cell population among NFAT family members (24, 34). The number of total thymocytes and the ratio of the $CD4^+CD8^+$ population in NFATx-disrupted mice are decreased, suggesting the important role of NFATx in thymocyte development (25). $CD4^+CD8^+$ cells undergoing thymic selection and single-positive cells in NFATx-disrupted mice express reduced levels of anti-apoptotic protein Bcl-2, thereby failing to support the survival of positively selected cells, leading to their apoptosis. However, the role of Bcl-2 in positive and negative selection is still under debate (41). We have shown here that the X-Δ(CRI·SP12) mutant of NFATx differentiated $CD4^+CD8^+$ cells into CD4 single-positive cells in the presence of PMA alone in the $CD4^+CD8^+$ cell line RLm6 and that this effect of the NFATx mutant was resistant to the calcineurin inhibitor FK506. We have shown that differentiation of $CD4^+CD8^+$ cells to CD4 single-positive cells could be induced by PMA and calcium ionophore treatment or by PMA treatment alone in the presence of constitutively active calcineurin (ΔCN) (26). The effect of the calcineurin mutant was inhibited by FK506. These data suggest that one of the crucial targets of calcineurin in the $CD4^+CD8^+$ stage is NFATx. Indeed, NFATx significantly contributes to an early rise in the DNA-binding activity of NFAT during the differentiation of $CD4^+CD8^+$ thymocytes *in vitro* (34). Therefore, NFATx should be involved in the differentiation of $CD4^+CD8^+$ thymocytes to CD4 single-positive cells during positive selection not only by up-regulating the expression of Bcl-2, but also by modulating the expression of the co-receptors, CD4 and CD8. This is the first evidence that shows the role of NFATx in the differentiation of $CD4^+CD8^+$ cells utilizing the NFATx molecule itself.

The NFAT family members and NF-κB family members show structural similarity and play crucial roles in the transcription of various genes, including many cytokine genes, upon activation of immune and inflammatory cells. In addition, both transcription factor families are suggested to be required for thymic development. The requirement of NF-κB activity for efficient positive selection has been shown by suppression of the activation of all NF-κB family proteins through the overexpression of the super-inhibitor IκB. IκB harbors mutations in the critical serine residues that are phosphorylated upon stimulation and that are required for IκB degradation. Thus, cells expressing IκB become resistant to the signal that activates all members of the NF-κB family. In IκB transgenic mice, positive selection of CD8 single-positive thymocytes is impaired (42). The overexpression of IκB in the $CD4^+CD8^+$ cell line DPK inhibits differentiation into CD4 single-positive cells induced by antigen stimulation (43). Although the transcription regulatory elements present in the CD8 cluster region and the CD4 locus have been extensively analyzed, NFAT or NF-κB sites have not been identified as critical regulatory elements. Utilizing mutant NFATx and the $CD4^+CD8^+$ cell line, we can shed light on the relationship between the transcription factors that directly regulate promoters and enhancers of the co-receptor genes and NFATx during thymic selection.

Acknowledgments—We thank Dr. K. Maruyama (Tokyo Medical and Dental University) for kindly supplying the pMKIT-Neo plasmid. We thank Drs. Yumiko Kamogawa and Esteban S. Masuda for helpful discussion. We also thank Miho Nagoya for technical assistance.

REFERENCES

1. Isakov, N., Mally, M. I., Scholz, W., and Altman, A. (1987) *Immunol. Rev.* **95,** 89–111
2. Dower, N. A., Stang, S. L., Bottorff, D. A., Ebinu, J. O., Dickie, P., Ostergaard, H. L., and Stone, J. C. (2000) *Nat. Immunol.* **1,** 317–321
3. Weiss, A., and Littman, D. R. (1994) *Cell* **76,** 263–274
4. Cantrell, D. (1996) *Annu. Rev. Immunol.* **14,** 259–274
5. Loh, C., Shaw, K. T., Carew, J., Viola, J. P., Luo, C., Perrino, B. A., and Rao, A. (1996) *J. Biol. Chem.* **271,** 10884–10891
6. Luo, C., Shaw, K. T., Raghavan, A., Aramburu, J., Garcia-Cozar, F., Perrino, B. A., Hogan, P. G., and Rao, A. (1996) *Proc. Natl. Acad. Sci. U. S. A.* **93,** 8907–8912
7. Shibasaki, F., Price, E. R., Milan, D., and McKeon, F. (1996) *Nature* **382,** 370–373
8. Zhu, J., and McKeon, F. (1999) *Nature* **398,** 256–260
9. Klemm, J. D., Beals, C. R., and Crabtree, G. R. (1997) *Curr. Biol.* **7,** 638–644
10. Beals, C. R., Sheridan, C. M., Turck, C. W., Gardner, P., and Crabtree, G. R. (1997) *Science* **275,** 1930–1934
11. Chow, C. W., Rincon, M., Cavanagh, J., Dickens, M., and Davis, R. J. (1997) *Science* **278,** 1638–1641
12. Zhu, J., Shibasaki, F., Price, R., Guillemot, J. C., Yano, T., Dotsch, V., Wagner, G., Ferrara, P., and McKeon, F. (1998) *Cell* **93,** 851–861
13. Masuda, E. S., Liu, J., Imamura, R., Imai, S. I., Arai, K. I., and Arai, N. (1997) *Mol. Cell. Biol.* **17,** 2066–2075
14. Masuda, E. S., Imamura, R., Amasaki, Y., Arai, K., and Arai, N. (1998) *Cell Signal.* **10,** 599–611
15. Beals, C. R., Clipstone, N. A., Ho, S. N., and Crabtree, G. R. (1997) *Genes Dev.* **11,** 824–834
16. Okamura, H., Aramburu, J., Garcia-Rodriguez, C., Viola, J. P., Raghavan, A., Tahiliani, M., Zhang, X., Qin, J., Hogan, P. G., and Rao, A. (2000) *Mol. Cell* **6,** 539–550
17. Sebzda, E., Mariathasan, S., Ohteki, T., Jones, R., Bachmann, M. F., and Ohashi, P. S. (1999) *Annu. Rev. Immunol.* **17,** 829–874
18. Anderson, G., Anderson, K. L., Conroy, L. A., Hallam, T. J., Moore, N. C., Owen, J. J., and Jenkinson, E. J. (1995) *J. Immunol.* **154,** 3636–3643
19. Jenkins, M. K., Schwartz, R. H., and Pardoll, D. M. (1988) *Science* **241,** 1655–1658
20. Gao, E. K., Lo, D., Cheney, R., Kanagawa, O., and Sprent, J. (1988) *Nature* **336,** 176–179
21. Urdahl, K. B., Pardoll, D. M., and Jenkins, M. K. (1994) *J. Immunol.* **152,** 2853–2859
22. Wang, C. R., Hashimoto, K., Kubo, S., Yokochi, T., Kubo, M., Suzuki, M., Suzuki, K., Tada, T., and Nakayama, T. (1995) *J. Exp. Med.* **181,** 927–941
23. Zhao, Y., and Iwata, M. (1995) *Int. Immunol.* **7,** 1387–1396
24. Amasaki, Y., Masuda, E. S., Imamura, R., Arai, K., and Arai, N. (1998) *J. Immunol.* **160,** 2324–2333
25. Oukka, M., Ho, I. C., de la Brousse, F. C., Hoey, T., Grusby, M. J., and Glimcher, L. H. (1998) *Immunity* **9,** 295–304
26. Kuwata, T., Asada, A., Ohoka, Y., Mukai, M., Miyaike, M., and Iwata, M. (1998) *Biochem. Biophys. Res. Commun.* **247,** 242–248
27. Ohoka, Y., Kuwata, T., Tozawa, Y., Zhao, Y., Mukai, M., Motegi, Y., Suzuki, R., Yokoyama, M., and Iwata, M. (1996) *Int. Immunol.* **8,** 297–306
28. Masuda, E. S., Naito, Y., Tokumitsu, H., Campbell, D., Saito, F., Hannum, C., Arai, K., and Arai, N. (1995) *Mol. Cell. Biol.* **15,** 2697–2706
29. Nakayama, E., Shiku, H., Takahashi, T., Oettgen, H. F., and Old, L. J. (1979) *Proc. Natl. Acad. Sci. U. S. A.* **76,** 3486–3490
30. Liu, J., Koyano-Nakagawa, N., Amasaki, Y., Saito-Ohara, F., Ikeuchi, T., Imai, S., Takano, T., Arai, N., Yokota, T., and Arai, K. (1997) *Mol. Biol. Cell* **8,** 157–170
31. Imamura, R., Masuda, E. S., Naito, Y., Imai, S., Fujino, T., Takano, T., Arai, K., and Arai, N. (1998) *J. Immunol.* **161,** 3455–3463
32. Miyatake, S., Sakuma, M., and Saito, T. (1997) *Eur. J. Immunol.* **27,** 1816–1823
33. Grynkiewicz, G., Poenie, M., and Tsien, R. Y. (1985) *J. Biol. Chem.* **260,** 3440–3450
34. Adachi, S., Amasaki, Y., Miyatake, S., Arai, N., and Iwata, M. (2000) *J. Biol. Chem.* **275,** 14708–14716

35. Jain, J., McCaffrey, P. G., Miner, Z., Kerppola, T. K., Lambert, J. N., Verdine, G. L., Curran, T., and Rao, A. (1993) *Nature* **365,** 352–355
36. Adachi, S., Kuwata, T., Miyaike, M., and Iwata, M. (2001) *Biochem. Biophys. Res. Commun.* **288,** 1188–1193
37. O'Keefe, S. J., Tamura, J., Kincaid, R. L., Tocci, M. J., and O'Neill, E. A. (1992) *Nature* **357,** 692–694
38. Park, S., Uesugi, M., and Verdine, G. L. (2000) *Proc. Natl. Acad. Sci. U. S. A.* **97,** 7130–7135
39. Shi, Y. F., Sahai, B. M., and Green, D. R. (1989) *Nature* **339,** 625–626
40. Aifantis, I., Gounari, F., Scorrano, L., Borowski, C., and von Boehmer, H. (2001) *Nat. Immunol.* **2,** 403–409
41. Williams, O., Mok, C. L., Norton, T., Harker, N., Kioussis, D., and Brady, H. J. (2001) *Eur. J. Immunol.* **31,** 1876–1882
42. Hettmann, T., and Leiden, J. M. (2000) *J. Immunol.* **165,** 5004–5010
43. Ochoa-Garay, J., Kaye, J., and Coligan, J. E. (1998) *J. Immunol.* **160,** 3835–3843